Available online at www.sciencedirect.com
ScienceDirect
Dyes and Pigments 75 (2007) 714–722
DYES and PIGMENTS
www.elsevier.com/locate/dyepig

Preparation, characterization and photocatalytic activity of a novel nanostructure composite film derived from nanopowder TiO_2 and sol–gel process using organic dispersant

Mohammad Hossein Habibi*, Mojtaba Nasr-Esfahani

Department of Chemistry, University of Isfahan, Hezarjirib, Isfahan 81746-73441, Iran

Received 25 January 2006; received in revised form 16 March 2006; accepted 25 July 2006
Available online 17 October 2006

Abstract

A novel sol–gel-derived titanium dioxide nanostructure composite has been prepared by spin-coating and investigated for the purpose of producing films. The processing of the composite sol–gel photocatalysts involved utilizing of precalcinated nanopowder titanium dioxide as filler mixed with sol and heat treated. The sol solution was prepared by adding titanium tetra isopropoxide ($Ti(OPr)_4$ or TTP) to a mixture of ethanol and HCl 35.5% (mole ratio TTP:HCl:EtOH:H_2O = 1:1.1:10:10), then a solution of 2 wt% methylcellulose was added and stirred at room temperature. Precalcinated TiO_2 nanopowder was dispersed in the sol and the prepared mixture was deposited on the microscope glass slide by spin-coating. The inhomogeneity problem in preparation of composite film which causes peeling off and cracking after calcination due to the shrinkage of the films with thermal treatment were overcome by using methylcellulose (MC) as a dispersant. The composite heat treated at approximately 500 °C has the greatest hardness value. Surface morphology of composite deposits by scanning electron microscopy (SEM) showed remarkable increase in the composite surface area. Evaluation of the adhesion and bonding strength between the coating and substrate was carried out by the scratch test technique. The minimum load which caused the complete coating removal, for composite thick film was 200 g/mm^2 which indicates a strong bond to the substrate. Photocatalytic activity of the composite film was evaluated through the degradation of a textile dye, Light Yellow X6G (C.I. Reactive Yellow 2) as a model pollutant and were compared with those of similar composite thick film without MC, thin film of TiO_2 and TiO_2 nanopowder. The results show that the photocatalytic activity and stability of the composite films are higher than those of nanopowder TiO_2. However, a remarkable increase in the composite surface and good mechanical integrity make this composite film a viable alternative for commercial applications.

Keywords: Photodegradation; Decolorization; Azo dye; Sol–gel; Light Yellow; Nanostructure; TiO_2 composite film; Methylcellulose

1. Introduction

Synthetic dyestuffs are extensively used in textile, printing industries, paper, and dye houses due to their ease of production, variety of colors, and fastness compared to natural dyes. Many commercially available dyes are known and approximately one million tons of these dyes are produced annually worldwide. It has been estimated that more than 10% of the total dyestuff used in dyeing processes is released into the environment [1–3]. Azo dyes are the largest group of dyes used for dyeing cotton fabrics in the industry [4]. Cotton is the most widely used fabric among all textiles, hence azo dyes are discharged frequently and in large quantities into the environment. The term azo dye is applied to synthetic organic colorants that are characterized by a nitrogen-to-nitrogen double bond [5]. Due to azo dyes poor exhaustion properties as much as 30% of the initial dye applied remains unfixed and end up in effluents. A necessary criterion for the use of these dyes is that they must be highly stable in light and during washing. They must also be resistant to microbial attack.

* Corresponding author. Tel.: +98 311 7932401; fax: +98 311 6687396.
E-mail address: habibi@chem.ui.ac.ir (M.H. Habibi).

0143-7208/$ - see front matter © 2006 Elsevier Ltd. All rights reserved.
doi:10.1016/j.dyepig.2006.07.032

Therefore, they are not readily degradable and are typically not removed from water by conventional chemical wastewater treatment systems. In the past, mainly chemical coagulation followed by activated sludge process was adopted to treat textile wastewaters. However, azo dyes due to their hydrophilic property are not removed by chemical coagulation. In general, physicochemical methods (coagulation and flocculation) produce large amounts of sludge which pose handling and disposal problems. On the other hand, due to the electron withdrawing nature of the azo bonds, they are not susceptible to aerobic oxidative catabolism [6] and hence are not removed in aerobic processes. Removing color from wastes is often more important than other colorless organic substances, because the presence of small amounts of dyes is clearly visible and influences the water environment considerably. Therefore, it is necessary to find an effective method of wastewater treatment in order to remove color from textile effluents.

In recent years, advanced oxidation processes have emerged as a promising technology for the degradation of organic pollutants. This includes heterogeneous photocatalytic systems such as a combination of large band gap semiconductor particles either dispersed in slurries or immobilized on films and UV light [7–11]. The advanced oxidation processes are costly in terms of installation, operation and maintenance costs but decolorization of azo dyes is achieved with the cleavage of the azo bond, thus rendering the dye colorless, with the formation of corresponding aromatic amines, which can be toxic and carcinogenic [12]. Because of their unique properties, a large number of semiconductor oxide films have been investigated during the past 60 years; among these titanium dioxide has gained much attention because of the strong photocatalytic abilities to purify pollutants in air and water under UV irradiation [13–17]. The use of semiconductor oxide particles as photocatalysts is well established and has shown great utility in the complete mineralization of organic pollutants. Titanium dioxide is well-known as a semiconductor, inexpensive, biocompatible, and non-toxic with photocatalytic activities and thus is applied in many fields such as for environmental purification, removal of harmful substances, and in the utilization of solar energy. However, the application of powder form TiO_2 is generally accompanied by complications arising from the need for filtration and separation of the powder from the treated liquid or gas. Particularly, TiO_2 having a crystal form of anatase is the most promising photocatalyst, despite its high photocatalytic activity. Much effort has been taken to improve the photocatalytic activity by modifying the surface or bulk properties of TiO_2, such as doping, codeposition of metals, surface chelation, and mixing of two semiconductors [18–20]. Titanium dioxide materials need to be synthesized with large surface areas and porous structures to achieve effective contact with reactants in the gas or liquid phase, since the photocatalytic or photochemical reactions occur on the surface of TiO_2. Nanometer-scaled titanium dioxide photocatalyst has attracted increasing attention due to its widespread environmental applications in water purification, antifogging, hazardous waste remediation, antidirtying, and water splitting reaction. The general reaction mechanism that leads to the overall reaction path to destroy pollutants is initiated by generation of photoelectron and photoholes that are uniformly distributed throughout the particle surface. The accumulation degree of negative charges also depends on the efficient transfer of photogenerated positive holes to hole scavengers in solution, due to efficient consumption of holes makes the recombination of photogenerated charge carrier to reduce, resulting in an efficient accumulation of electrons. One of the most important factors that control the high photocatalytic activity is the kinetics of recombination process [21–23].

Recently, considerable interest has been focused on sol–gel-derived nanocomposite films and powders which have been considered as effective photocatalysts. It has been shown that properties of composites obtained often cannot be considered as a simple superposition of the properties of individual components due to strong surface interactions between the closely packed nanoparticles in the binary oxide systems. Sol–gel processing is one of the most common methods to produce photocatalyst TiO_2 in both forms – coatings and powder – and provides many advantages over the conventional methods including the possibility to control a number of determining parameters of the final product; homogeneity, purity, microstructure and sintering temperature are among the many advantages of sol–gel processing methods. The final product could be shaped into various forms such as fibers, monoliths, thin and thick film coatings, and powders. However, there are a number of critical drawbacks regarding sol–gel processing, including high shrinkage of the resulting product (film or monolith) during drying and heat treatment [24–29]. Sintering colloidal TiO_2 paste is one of the simplest ways to fabricate porous films, but due to low mechanical integrity to substrate is not a good candidate for large scale applications such as photodegradation of organic compounds. In addition, nanostructured TiO_2 film has been made by a variety of techniques such as e-beam evaporation, magnetron sputtering technique, anodization, chemical vapour deposition and sol–gel technique. The sol–gel technique has attracted more attention due to low process cost, low temperature of heat treatment and wide possibility to vary film properties by changing the composition of the solution. Numerous literature reports on the fabrication of TiO_2 thin films by sol–gel dip coating technique using many types of titanium alkoxides as precursors. The major disadvantage is shrinkage of the resulting product (film or monolith) during drying and heat treatment. Since thin (<200 nm) films may exhibit relatively low photoefficiency and since thicker films may not possess sufficient mechanical integrity the use of polymerized materials to improve homogeneity, increase surface area and improve adhesion/cracking after calcination has been explored. A processing method to produce sol–gel derived composite-coatings of photocatalytic TiO_2 without any dispersant has also been reported [30–40].

In continuation of our ongoing programme to develop thin solid films for photocatalytic and photoelectrocatalytic purposes [41–43], in the present study we report the preparation of a novel composite film derived from thin film and nanopowder TiO_2 using methylcellulose as dispersant on slide glass by

sol–gel single spin-coating process for photocatalytic decolorization of textile dyes. MC is a water-soluble long chain polymer which is suitable for use in sol–gel processing with high water content. Another advantage is that MC belongs to nonionic cellulose ether, which is substantially free of substance that can induce crystallization of titania during any of the coating formation and densification process steps. Using MC as a dispersant we have solved some problems such as inhomogeneity and defects that may be introduced by peeling off and cracking after calcination due to the shrinkage of the films with thermal treatment. We have used TiO_2 nanopowder with high surface area for prevention of decreasing final surface area in composite thick film, due to densification and crystal growth of filler and matrix in composite. The photocatalytic properties of this film toward Light Yellow X6G (C.I. Reactive Yellow 2) degradation were investigated and compared with similar composite thick film without MC, thin film of TiO_2 and TiO_2 nanopowder. We have examined the effect of some parameters such as dye concentration and solution pH on the photodegradation rate.

2. Experimental

2.1. Materials

Standard ethanol solution ($M = 46.07$ g/mol, purity $\approx 99.8\%$) was purchased from Fluka Chemical. Hydrocholoric acid ($M = 36.5$ g/mol, purity $\approx 35.5\%$) was supplied by Merck. Titanium tetra isopropoxide ($Ti(OPr)_4$ or TTP) (Aldrich, 97%), the precursor, was used without further purification. TiO_2 nanopowder, anatase in crystalline form, has a surface area of about 190–290 m^2/g, particle size of 15 nm and was obtained from Aldrich. Methylcellulose (low substitution) was obtained from Harris Chemical. Light Yellow X6G (C.I. Reactive Yellow 2, M.W. = 872.5 g/mol) textile dye was obtained from Youhao (China) and the chemical structure is shown in Fig. 1. The water used in the experiments was double distilled and deionized.

2.2. Preparation of composite film

2.2.1. Preparation of sol

Titania solution containing high mole ratio of water suitable for mixing with organic binder material MC was prepared using the following procedure (Fig. 2). Titania matrix solution was prepared by typical controlled hydrolysis process. The sol solution was prepared by adding 5 ml TTP to a 50 ml beaker containing a mixture of 10 ml ethanol and 1.8 ml HCl 35.5%

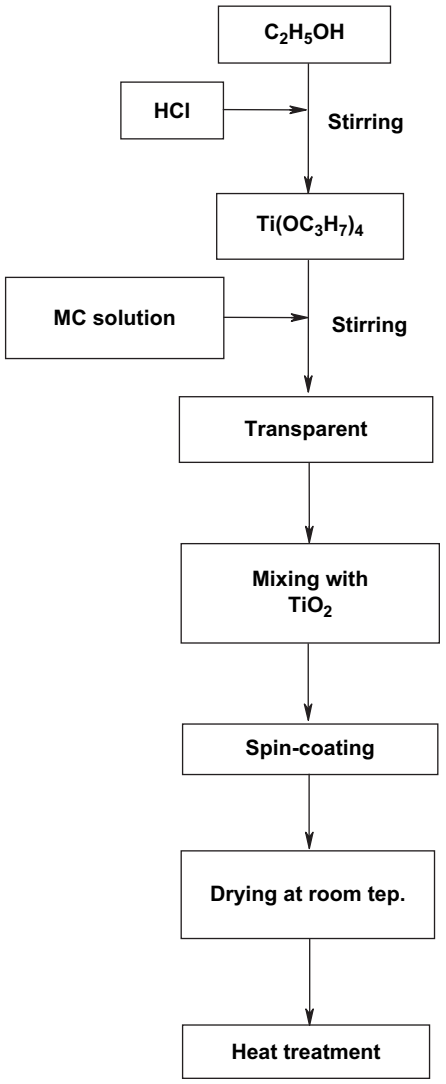

Fig. 2. Preparation of composite TiO_2 thick film coating.

that had been mixed for 5 min. The mixture was vigorously stirred during addition and for a further 120 min after addition of the precursor at room temperature. Methylcellulose 2 wt% solution was prepared using MC and double distilled water. Then these two solutions (titanium precursor and MC solution) were added dropwise and stirred overnight at room temperature. The molar ratio was TTP:HCl:EtOH:H_2O, 1:1.1:10:10.

2.2.2. Preparation of composite films

Precalcined TiO_2 nanopowder was used as filler mixed with the sol (5% of sol). TiO_2 nanopowder was dispersed in the sol

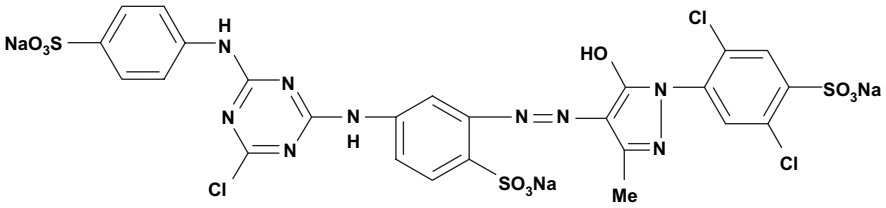

Fig. 1. Chemical structure of commercial diazo dye, Light Yellow X6G (C.I. Reactive Yellow 2).

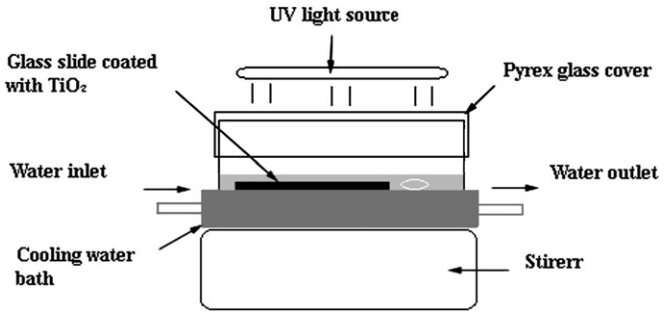

Fig. 3. Schematic diagram of photoreactor.

and the prepared mixture was deposited on the microscope glass slide (75 mm × 25 mm × 1 mm) by homemade spin-coating. Generally, the coating process can be divided into three steps: (a) the substrate ultrasonically cleaned in ethanol prior to use, (b) the substrate attached to a prefixed speed and the mixture poured on it to distribute evenly on the substrate by the centrifugal force, the liquid in excess being throw off and (c) the solvent evaporates. The speed and the deposition time in step (b) are fixed: 30 s at 2000 rpm. The dried films were heated in a muffle furnace to 500 °C at a heating rate of 5 °C min^{-1} and maintained at this temperature for 60 min and cooled to room temperature at a similar rate. These composite films were used for photocatalytic reactions, otherwise the photocatalysts were stored in the dark to avoid pre-activation by room light or sunlight.

2.3. Characterization techniques

The phase composition of photocatalyst was studied by the powder and plate XRD technique. The X-ray diffraction patterns were obtained on a D8 Advanced Bruker X-ray diffractometer using Cu Kα radiation at a scan rate of 0.03 2θ S^{-1}. The accelerating voltage and the applied current were 40 kV and 35 mA, respectively. The crystallite size was calculated by X-ray line broading analysis using Scherrer formula.

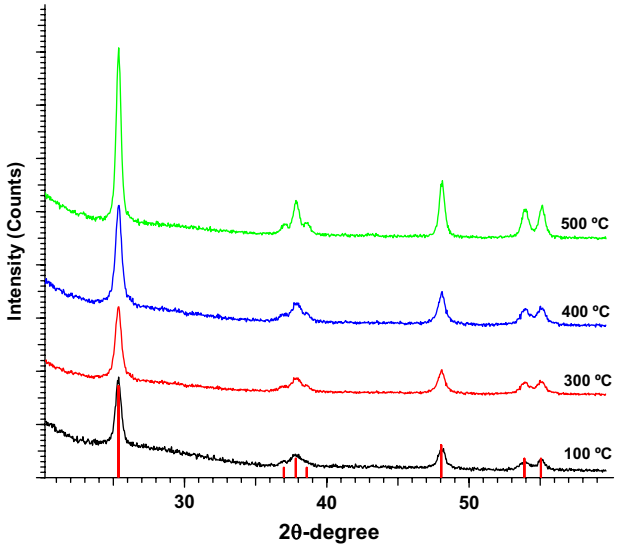

Fig. 4. XRD patterns for TiO_2 composite thick film with MC by one time spin-coating and heat treated at different temperatures.

In order to examine the thermal properties of the composite materials, a METTLER TA5 was used for TGA measurement of the gel powder of the composite materials obtained from mixture of sol and TiO_2 nanopowder poured into a Petri dish by drying at room temperature for about 10 days. Samples of 0.01 mg crushed powder are put into an Al_2O_3 crucible for TGA. The heating rate is 5 °C/min in flowing air. The recorded temperature range is from room temperature to 700 °C. A similar test was done for MC.

Scratch coating adhesion tests were performed in order to evaluate the mechanical integrity of the deposited coatings on the glass slide substrates using a Motorised Clemen scratch tester (equipped with a tungsten carbide ball tool, 1 mm). All the coatings were deposited by spin-coating method on the substrates with the same controlled thickness. Scratches were made under variable applied load (force) from 0 to 1000 g, for a maximum length of 50 mm. The resulting damage to the coatings was visually observed by the optical microscope to determine the point of coating adhesive failure (i.e. the point at which the indenter starts to scratch the substrate surface). The load at this point was considered as indicative of the coating resistance to scratch failure.

The stability of TiO_2 suspensions was investigated by sedimentation rate measurements. The settling experiments were performed using 50 ml measuring cylinders with the same diameter (~20 mm). The prepared suspension was poured into cylinders to the exact height of 20 cm and the height of sedimentation was measured with time.

Microstructure of the composite films was observed by Scanning Electron Microscope (SEM) Philips XL30, at a voltage of 20 kV (sputtered by gold).

2.4. Photoreactor and photocatalytic measurements

To evaluate the catalytic activity of composite film, the photodegradation of a well-known organic azo dye X6G (C.I. Reactive Yellow 2) is investigated as a simple model compound (Fig. 1) under UV irradiation.

The experiments were carried out in a custom made photocatalytic oxidation reactor measured by 40 cm × 15 cm × 15 cm (Fig. 3). One TiO_2/glass with one time spin-coating (75 mm × 25 mm × 1 mm) was used as photocatalyst and irradiated with two 8 W UVA ($\lambda = 365$ nm) at a distance of 5 cm from the top of the model solution. In a typical experiment, 10 ml of each dye solution with initial concentration of 12 ppm was used. The solution was stirred continuously and a constant-temperature water bath was maintained at 25 °C. Four milliliters of the sample was taken at regular time intervals during irradiation and analyzed by a double beam UV–vis spectrophotometer (Varian Cary 500 Scan) to measure the concentration of dye at 400.0 nm and 270.0 nm. Dye solution (10 ml) was also photolyzed in the presence of a similar composite thick film without MC or slurry suspension of TiO_2 nanopowder (160 ppm) under the same conditions as a reference.

3. Results and discussion

3.1. Preparation of sol

The typical sol, presented in this study, with the TTP:H_2O:EtOH:HCl molar ratio of 1:10:10:1.1, was found to be most suitable for dissolving MC and dispersion of TiO_2. Deferent compositions of TiO_2 sol were prepared by altering the molar ratio of TTP:H_2O:HCl. Increasing the water content and dilution of the sol system may retard the gelation. The process was exothermic and the pH of the solution was about 2–3 and MC acts as a dispersant and it may retard the gelation.

3.2. Stability of TiO_2 suspension

To produce a homogenous suspension of TiO_2 precalcined particles in the sol, for composite thick film preparation, it was essential to study the interaction of media (sol) and the filler (TiO_2 particles), in terms of the stability of the suspension. By controlling the interparticle forces, the colloidal suspension can be prepared in the dispersed or the flocculated forms, which dictated its stability by time [44]. A rise in potential energy resulting from steric interactions between particle surfaces coated with adsorbed polymeric species is one of the ways for producing a stable suspension. Stability of TiO_2 suspension was investigated by sedimentation rate measurement. Various suspensions with different concentrations of TiO_2-anatase nanopowder in sol with MC and without MC were prepared in the range of 5–10 wt%. Settling rate of the TiO_2 nanopowder in the sol without MC with 5% and 10% concentrations was very low (1 h and 30 min, respectively). The beginning of the settlement of the TiO_2 nanopowder in the sol with MC with 5% and 10% concentrations varies from 3 days for lowest concentration suspension to 10 h for the highest one (10 wt%). There is less repulsive force between the TiO_2 particles in a more concentrated suspension and the settlement of the particles occurs faster. The repulsive force between the TiO_2 particles is increased by using MC in the sol and the slower rate in settlement of the particles.

3.3. XRD characterization of TiO_2 photocatalyst

The principal goal of carrying out XRD analysis was to identify the TiO_2 polymorphs and their crystalline phases. Fig. 4 shows the X-ray diffraction patterns of composite film TiO_2 nanopowder and MC when heat treated at different temperatures. The 2θ angles of the reflections corresponding to the basal spacing of the TiO_2/glass were 25.28, 37.02, 37.80, 38.82, 48.05, 53.9, and 55.06 for peaks 1, 2, 3, 4, 5, 6, and 7, respectively. These values corresponded to the d (Å) values for all the peaks of TiO_2/glass from 100 to 500 °C with the standard JCPDS values 3.52, 2.43, 2.38, 2.33, 1.89, 1.70, and 1.67 nm, respectively, showing existence of anatase phase TiO_2. The intensity of TiO_2 peak increases when the sample was annealed at higher temperature. This shows that annealing has a significant effect on the TiO_2/glass crystallinity. Higher intensity of TiO_2 peak indicates that the availability of TiO_2 compound increases as well, especially in the conversion of amorphous TiO_2 derived from the sol into the active anatase TiO_2. Our result is in good agreement with the one reported by Keshmiri et al. [36]. Harizanov and Harizanova [45] have observed that exothermic peaks of TiO_2 gel, localized between 250 and 500 °C show the process of oxidation of the organic residuals and crystallization of TiO_2-anatase structure. Similarly, Mazzarino et al. [46] also found the conversion of amorphous titania thin film into the active crystallite structure of the catalyst (anatase) by thermal treatment at 500 °C.

Fig. 5 demonstrates that the diffractogram of the dried TiO_2 powder showed very clear and intense peaks of anatase compared with the XRD pattern for TiO_2 composite film calcined at 100 °C (as expected the clean glass show only a broad band at a d value of 3.50 nm).

The average crystallite sizes of TiO_2 were calculated by Scherrer's equation using the full width at half maximum (FWHM) of the X-ray diffraction peaks at $2\theta = 25.3$. As shown in Table 1, typical values of anatase crystallite size have been calculated to be in the range of 15.5–16.5 nm for the synthesized TiO_2 particles on glass. The size of the anatase crystallites in the composite thick films, either with or without MC, follows the size range of the crystallites in the filler powder (TiO_2 nanopowder). Therefore, the size of the TiO_2 crystallites, derived from the sol, does not affect the size of final crystallites.

In order to examine the thermal properties of the composite materials, the gel powder of the composite materials obtained from the mixed sol solution with TiO_2 nanopowder was tested. For comparison a powder of MC was also tested. The results show that weight loss occurs at three stages, namely, below 200 °C, between 200 and 280 °C and from 280 to 450 °C. In the first region (below 200 °C), the weight loss is believed to be a result of the evaporation of water and the thermal decomposition of the remnant organic solvents. Between 200 and

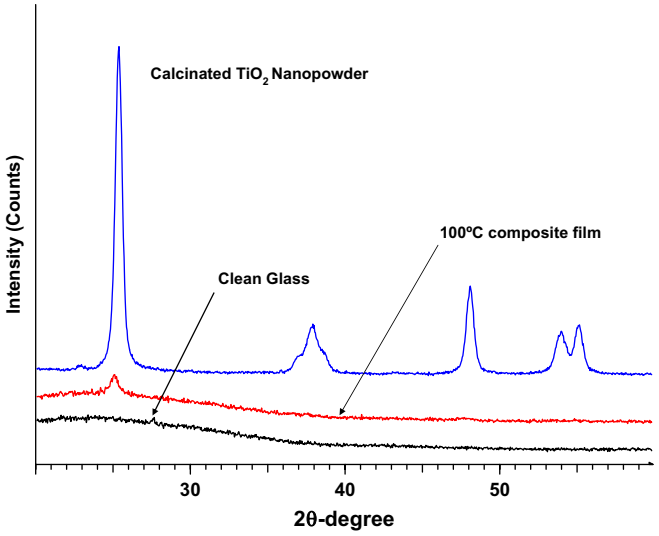

Fig. 5. XRD spectrum of clean glass, dried TiO_2 nanopowder, and TiO_2/glass with one time spin-coating at 500 °C.

Table 1
Physical and chemical characteristics of different TiO_2 photocatalysts heat treated for 1 h at 500 °C

Material	Scratch adhesion (g/mm^2)	Rate constant (min^{-1})	$t_{1/2}$ (min)	Particle size (nm)
TiO_2 nanopowder	~0	0.0547	12.67	16.3
Composite thick film with sol and without MC	150	0.0231	30	16.4
Composite thick film with sol and MC	200	0.0277	25	16.3

280 °C, the weight loss is attributed to the carbonization or the combustion of organic compounds such as MC in the composite. Between 280 and 450 °C or more, the weight losses are probably ascribed to the evaporation of physically absorbed water and further combustion of the remaining organic additives. Therefore, MC in the final product completely disappeared.

3.4. Surface morphology

Fig. 6 shows SEM image of the surfaces of heat treated composite TiO_2 film at 500 °C for 60 min with or without MC as dispersant. Composite film with MC was more homogenous and uniform than the composite film without MC. As shown in Fig. 6b, the composite film without MC has ununiform surface with large tracks. Introducing the MC in the composite has affected the surface morphology and roughness of films.

The annealing process at 500 °C resulted in a remarkable increase in the composite surface area and stronger bond to the substrate (according to the mechanical test results). The diameter of the pores, created in composite film was increased and the microcracks on the composite film are evidence for the development of more porous structure.

3.5. Scratch adhesion test

The scratch test technique was used for the adhesion and bonding strength between the coating and substrate. The results showed a sharp increase in the adhesion and bonding strength between the coating and substrate composite film and substrate using MC as dispersant. The minimum load which caused complete coating removal, for composite thick films with and without MC is presented in Table 1.

3.6. Photocatalytic activity

Photocatalytic experiments were carried out to evaluate the films as a possible material for water pollutant purification. The photocatalytic activity of the composite thick films was estimated by discoloration and mineralization of a model textile dye, namely X6G, a characteristic member of azo dyes. A preliminary test was carried out in the dark using the prepared photocatalyst. The results confirmed that the removal of dye was insignificant for the mentioned condition. It must be stressed that total removal of the model pollutant was not due to the effect of photodegradation alone. A small portion of the removal efficiency was attibutable to the rapid attainment of adsorption equilibrium of the dye onto TiO_2 composite/glass. The surface charge property of TiO_2 films changes with the solution pH. For nanosized TiO_2, the pH_{zpc} (zero point charge) is known to be 5.1 [47]. Therefore, since the roughness of the composite film is very high for reduction absorption effect we regulate the pH of the solution to 5.1. At this pH, adsorption of the dye onto TiO_2 composite/glass was negligible. An aqueous solution of X6G dye without photocatalyst was irradiated for 12 h to check the pollutant stability under UV illumination. The results illustrated in Fig. 7 (□) revealed that X6G remained intact throughout the irradiation time.

The presence of the TiO_2 materials, in slurry (Fig. 7 (▲)), composite thick film without MC (Fig. 7 (■)) or composite thick film with MC (Fig. 7 (●)) resulted in an effective photocatalytic decomposition of the azo dye. To a first approximation, the three modes of degradation (i.e. slurry TiO_2 and two composite thick films) seem to proceed through the same intermediates (Fig. 7). It is worth to mention that the slurry and composite films consist approximately of the same material (TiO_2 nanopowder).

Under the experimental conditions used, the photocatalytic curves seem to follow first-order reaction kinetics. Generally, the photodegradation rates of chemical compounds on

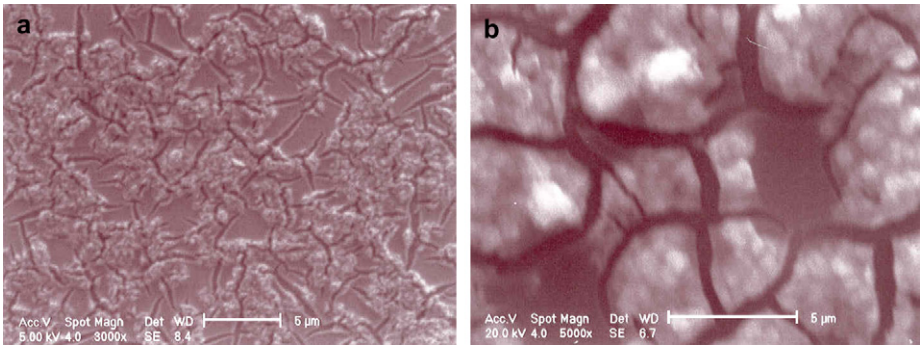

Fig. 6. SEM images of composite TiO_2 film after heat treatment at 500 °C with MC (a) and without MC (b).

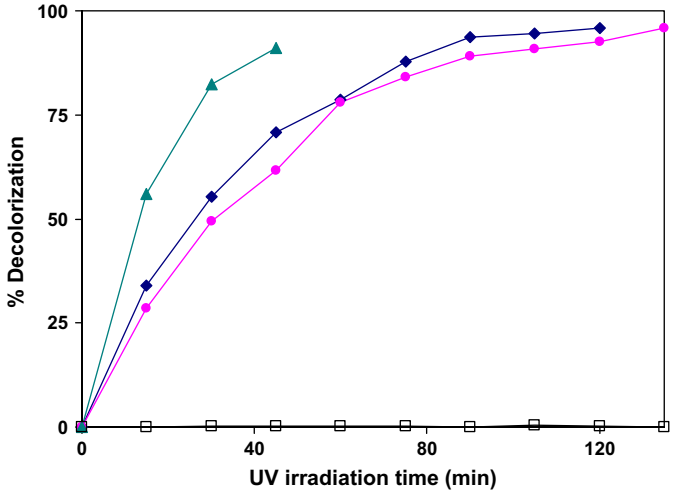

Fig. 7. Decomposition of X6G (12 ppm) dye solution without photocatalyst (□), in the presence of slurry TiO_2 nanopowder (160 ppm) solution (▲), composite thick film without MC (■) and composite thick film with MC (●).

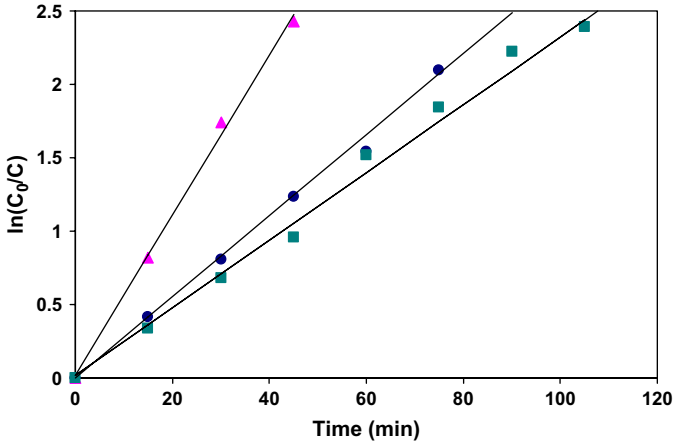

Fig. 8. The kinetic data for photocatalytic degradation of X6G in the presence of slurry nanopowder TiO_2 (160 ppm) solution (▲), composite thick film without MC (■) and composite thick film with MC (●).

semiconductor surfaces follow the Langmuir–Hinshelwood model [48,49].

$$R = \mathrm{d}C/\mathrm{d}t = k_r\theta = k_rKC/(1+KC) \quad (1)$$

where k_r is the reaction rate constant, K is the absorption coefficient of the reaction, and C is the reactant concentration. The values of k_r and K are used to explain the coefficients defining the rate determining reaction events and pre-equilibrium adsorption within an adsorbed monolayer at the oxide surface and the aqueous solution interface. The effect of light intensity is also incorporated in k_r and K especially expresses the equilibrium constant for fast adsorption–desorption processes between surface monolayer and bulk solution [48]. Integration of Eq. (1) yields the following equation:

$$\ln\left(\frac{C_0}{C}\right) + K'(C_0 - C) = k_rKt \quad (2)$$

When the initial concentration C_0 is small, Eq. (2) changes to Eq. (3), which expresses a pseudo-first-order reaction kinetic regime.

$$\ln\left(\frac{C_0}{C}\right) = k_rKt = kt \quad (3)$$

yielding half-life, $t_{1/2}$ (in min) is

$$t_{1/2} = \frac{0.693}{k} \quad (4)$$

where k is the pseudo-first-order reaction rate constant, $k = k_rK$ in min^{-1}. Two plots of $\ln(C_0/C)$ versus time for the dye in the optimized conditions were linear (Fig. 8), suggesting that the photodegradation reaction follows the pseudo-first-order reaction kinetics. The pseudo-first-order reaction rate constants and half-life parameters for the azo dye are listed in Table 1. To a reasonable approximation, the slope of the photodegradation profiles corresponds to a relative pseudo-first-order rate constant (min^{-1}).

To compare the photocatalytic degradation of composite TiO_2 film with nanopowder slurry, the dye solution (10 ml) was also photolyzed in the presence of a suspension (dispersion) of TiO_2 nanopowder with the same weight as film (0.0016 g = 160 ppm) and the results are represented in Fig. 8 (▲). The rate constant for the slurry is greater than that of the two thick films, showing a considerably higher efficiency as photocatalyst. According to kinetic models for photocatalytic degradation of organic contaminants over titania thin film catalysts, the rate of degradation is limited by liquid-film transfer, diffusion, adsorption or a combination of these three factors. It is worth mentioning that on TiO_2 film samples, only part of the catalyst is exposed to the pollutant solution and can therefore be photocatalytically active. As a result, a decrease in the overall photocatalytic performance of thick films compared to slurry solution is expected. In fact, one must have in mind that during the thermal treatment of composite film no significant change in the structural modification was observed, this difference can be easily understood if one considers that the photocatalytic process is a surface and not a volume or mass phenomenon. The active photocatalyst is the illuminated TiO_2 material, which can be in contact with the organic dye, and in the case of the film this only concerns its external surface. As the TiO_2 nanopowder surface area is very high (190–290 m^2/g) with use of this kind of TiO_2, we tried to increase this surface area in the composite thick film. Fig. 8 (■ and ●) presents rate constants for composite thick films without and with MC. The rate constant for the composite thick film with MC is greater than that of the composite thick film without MC, showing a considerably higher efficiency as photocatalyst. Figs. 7 and 8 show how photoefficiency can be significantly improved by use of a porous composite thick film in addition to other advantages such as unnecessary to separate TiO_2 powder at the end of photodegradation. The increasing surface area of composite thick film enhanced the photoactivity of the catalyst by increasing the reactive surface area.

Therefore, by introducing MC, which results in a porous body after calcination (as is seen in Fig. 6), we could enhance rate constant of photodegradation of X6G.

4. Conclusion

A nanostructure composite film with high structural integrity and photocatalytic efficiency was developed through a novel method using nanopowder TiO_2, sol–gel process and organic dispersant. The photocatalyst is designated for use in degradation of a model dye pollutant in water. The processing of the composite sol–gel photocatalysts involved utilizing precalcinated nanopowder titanium dioxide as filler mixed with the sol and heat treated. The sol solution was prepared by adding titanium tetra isopropoxide to a mixture of ethanol and HCl, then a solution of methylcellulose was added and stirred at room temperature. Precalcinated TiO_2 nanopowder was dispersed in the sol and the prepared mixture was deposited on the microscope glass slide by spin-coating. The inhomogeneity and defects problems for preparation of composite film which causes peeling off and cracking after calcination due to the shrinkage of the films with thermal treatment were overcome by using methylcellulose (MC) as a dispersant. The composite film showed that the photocatalytic activity and stability of the composite films are higher than those of nanopowder TiO_2. However, a remarkable increase in the composite surface and good mechanical integrity make this composite film a viable alternative for commercial applications.

Acknowledgments

The authors wish to thank the University of Isfahan for financially supporting this work.

References

[1] Claus H, Faber G, Konig H. Redox-mediated decolorization of synthetic dyes by fungal laccases. Appl Microbiol Biotechnol 2002;59:672–8.
[2] Selvam K, Swaminathan K, Keo-Sang C. Microbial decolorization of azo dyes and dye industry effluent by *Fomes lividus*. World J Microbiol Biotechnol 2003;19:591–3.
[3] Maguire RJ. Occurrence and persistence of dyes in a Canadian river. Water Sci Technol 1992;25:265.
[4] Zhang C, Fu C, Bishop L, Kupferle M, FitzGerald S, Jiang H, et al. Transport and biodegradation of toxic organics in biofilms. J Hazard Mater 1995;41:267–85.
[5] Chudgar RJ. Dyes, application and evolution. In: Kroschwits JI, Howe-Grant M, editors. Kirk–Othmer encyclopedia of chemical technology, vol. 3. New York: John Wiley & Sons Inc.; 1991. p. 821–75.
[6] Pagga U, Taeger K. Development of a method for adsorption of dyestuffs on activated sludge. Water Res 1994;28(5):1051–7.
[7] Legrini O, Oliveros E, Braun AM. Chem Rev 1993;93:671–8.
[8] Hoffmann MR, Martin ST, Choi W, Bahnemann DW. Chem Rev 1995;95:69–96.
[9] Ollis DF, Al-Ekabi H, editors. Photocatalytic purification and treatment of water and air. Amsterdam: Elsevier Science Publishers; 1993.
[10] Turchi CS, Ollis DF. J Catal 1990;122:178–92.
[11] Fox MA, Dulay M. Chem Rev 1993;93:341–57.
[12] Wuhrmann K, Mechsner K, Kappeler T. Investigation on rate-determining factors in the microbial reduction of azo dyes. Eur J Appl Microbiol Biotechnol 1980;9:325–38.
[13] Buechler KJ, Noble RD, Koval CA, Jacoby WA. Ind Eng Chem Res 1999;38:892–6.
[14] Konstantinou IK, Sakellarides TM, Sakkas VA, Albanis TA. Environ Sci Technol 2001;35:398–405.
[15] Habibi MH, Hassanzadeh A, Mahdavi S. The effect of operational parameters on the photocatalytic degradation of three textile azo dyes in aqueous TiO_2 suspensions. J Photochem Photobiol A Chem 2005; 172:89–96.
[16] Habibi MH, Vosoghian H. Photocatalytic degradation of some organic sulfides as environmental pollutants using titanium dioxide suspension. J Photochem Photobiol A Chem 2005;172:45–52.
[17] Habibi MH, Tangestaninejad S, Yadollahi B. Photocatalytic mineralization of mercaptans as environmental pollutants in aquatic systems using TiO_2 suspensions. Appl Catal B Environ 2001;33(1):57.
[18] Ollis DF, Al-Ekabi H, editors. Photocatalytic purification and treatment of water and air. Amsterdam: Elsevier; 1993.
[19] Yanagisawa K, Yamamoto Y, Feng Q, Yamasaki N. J Mater Res 1900;13(4):825.
[20] Chan CK, Porter JF, Li Y-G, Guo W, Chan C-M. J Am Ceram Soc 1999;83(3):566.
[21] Yu JC, Yu J, Ho W, Jiang Z, Zhang L. Chem Mater 2002;14:3808.
[22] Peiro A, Peral J, Domingo C, Domenech X, Ayllon J. Chem Mater 2001;13:2567.
[23] Yasumori A, Shinoda H, Kameshima Y, Hayashi S, Okada K. J Mater Chem 2001;11:1253.
[24] Woolfrey JL, Bartlett JR. In: Klein LC, Pope EJA, Sakka S, Woolfrey JL, editors. Sol–gel processing of advanced materials. The American Ceramic Society; 1998. p. 3.
[25] Mackenzie JD. In: Hench LL, Urlich DR, editors. Science of ceramic chemical processing. Wiley; 1986. p. 113.
[26] Segal D. J Mater Chem 1997;7:1297.
[27] Bouquin O, Blanchard N, Colombian Ph. In: Vincenzini P, editor. High tech ceramics. Amsterdam: Elsevier; 1987. p. 717.
[28] Livage J, Beteille F, Roux C, Chatry M, Davidson P. Acta Mater 1998;46:743.
[29] Hench LL, West JK. The sol–gel process. Chem Rev 1990;90:33–72.
[30] Scherer GW. J Am Ceram Soc 1990;73:3.
[31] Scherer GW. J Non-Cryst Solids 1987;92:375.
[32] Ring TA. Fundamentals of ceramic powder processing and synthesis. Academic Press; 1996. p. 349.
[33] Brinker CJ, Scherer GW. Sol–gel science – the physics and chemistry of sol–gel processing. Academic Press; 1990. p. 675.
[34] German RM. Sintering theory and practice. New York: Wiley; 1996. p. 67.
[35] Arabatzis IM, Antonaraki S, Stergiopoulos T, Hiskia A, Papaconstantinou E, Bernard MC, et al. Preparation, characterization and photocatalytic activity of nanocrystalline thin film TiO_2 catalysts towards 3,5-dichlorophenol degradation. J Photochem Photobiol A Chem 2002;149:237–45.
[36] Keshmiri M, Troczynski T, Mohseni M. Development of novel TiO_2 sol–gel derived composite and its photocatalytic activities for trichloroethylene oxidation. Appl Catal B Environ 2004;53:209–19.
[37] Bange K, Ottermann CR, Anderson O, Jeschkowsky U, Laube M, Feile R. Investigations of TiO_2 films deposited by different techniques. Thin Solid Films 1991;197:279–85.
[38] Hossein-Babaei F, Keshmiri M, Kakavand M, Troczynki T. A resistive gas sensor based on undoped p-type anatase. Sens Actuators B 2005;110:28–35.
[39] Chatterjee D, Dasgupta S. Visible light induced photocatalytic degradation of organic pollutants. J Photochem Photobiol A Photochem Rev 2005;6:186–205.
[40] Chen W, Zhang J, Fang Q, Li S, Wu J, Li F, et al. Sens Actuators B 2004;100:195–9.
[41] Habibi MH, Talebian N. Photocatalytic degradation of an azo dye X6G in water: a comparative study using nanostructured indium tin oxide and titanium oxide thin films. Dyes Pigments 2007;73:186–94.
[42] Habibi MH, Talebian N. The effect of annealing on structural, optical and electrical properties of nanostructured tin doped indium oxide thin films. Acta Chim Slov 2005;52:53–9.

[43] Hassanzadeh A, Habibi MH, Zeini Isfahani A. Study of electronic structure of tin-doped In_2O_3 (ITO) film deposited on glass. Acta Chim Slov 2004;51:507.
[44] Lewis JA. Colloidal processing of ceramics. J Am Ceram Soc 2000;83(10):2341–59.
[45] Harizanov O, Harizanova A. Development and investigation of sol–gel solutions for the formation of TiO_2 coatings. Sol Energy Mater Sol Cells 2000;63:185–95.
[46] Mazzarino I, Piccinini P, Spinelli L. Degradation of organic pollutants in water by photochemical reactors. Catal Today 1999;48:315–21.
[47] Yang TC-K, Wang S-F, Tsai SH-Y, Lin S-Y. Appl Catal B Environ 2001;30:293–301.
[48] Houas A, Lachheb H, Ksibi M, Elaloui E, Guillard C, Herrmann J. Appl Catal B Environ 2001;31:145–57.
[49] Fujishima A, Rao TN, Tryk DA. J Photochem Photobiol 2000;C1: 1–21.